Nuclear Science and Technology, November 2000.

NEUTRON CROSS SECTION EVALUATIONS FOR ^{238}U UP TO 150 MeV

A. V. Ignatyuk, V. P. Lunev, Yu. N. Shubin, E.V. Gai, N. N. Titarenko

Institute of Physics and Power Engineering, 249020 Obninsk, Russia

A.Ventura

ENEA, Nuclear Data Center and INFN, Bologna Section, 40129 Bologna, Italy

W.Gudowski

Royal Institute of Technology, 100-44 Stockholm, Sweden

Abstract: Investigations aimed at the development of neutron cross section evaluations for ^{238}U at intermediate energies are briefly described. The coupled-channels optical model is used to calculate the neutron total, elastic and reaction cross sections and the elastic scattering angular distributions. Evaluations of the neutron and charged particle emission cross sections and of the fission cross sections are obtained on the basis of the statistical description that includes direct, pre-equilibrium and equilibrium mechanisms of nuclear reactions. The Kalbach parametrization of angular distributions is used to describe the double-differential cross sections of emitted neutrons and charged particles in ENDF/B-VI format.

I. INTRODUCTION

In order to develop main concepts of the accelerator-driven power systems and the corresponding nuclear waste management it is necessary to know nuclear data on spectra and reaction cross sections for structural materials, fissioning actinides and the most important fission products in a very broad energy range. In practice, the energy interval from thermal energies to a few thousand MeV should be covered [1]. The status of available nuclear data differs strongly for the energy regions below and above of 20 MeV. Huge efforts have been made to create libraries of evaluated neutron data (ENDF/B, JENDL, BROND etc.), for the low energy region. In spite of some differences between the evaluations, most data are reasonable enough and their accuracies satisfy requests of major current applications. For energies higher than 20 MeV data are rather scarce and are not systematized yet.

A lack of experimental data has to be compensated by the development of reliable calculation methods. The codes based on the intranuclear cascade model combined with the evaporation model have been successfully applied for energies above a few hundred MeV [2-4]. At lower energies, however, nuclear structure effects are so prominent that their description requires more detailed consideration of competitive reaction mechanisms. Therefore, it was decided that the energy region from 20 to 150 MeV requires special consideration and the evaluated data files for this region should be prepared for the most important structural and fissile materials in the same manner as for the energy region below 20 MeV [1]. In accordance with that, the evaluated data files for about 30 of the most important structural and shielding materials were extended in the ENDF/B-VI library up to 150 MeV by the Los Alamos group [5]. Some attempts to prepare similar evaluations for actinides were made by this group, too [6], but they were limited to neutron elastic scattering and neutron production cross sections, mainly for energies below 100 MeV. Fission cross sections, charged particle yields, and fission neutron yields were not included in the files prepared on the basis of the evaluations. These important shortcomings of evaluations, as well as some unrealistic fluctuations obtained in the neutron production cross sections were already pointed out by the authors [6].

The list of first priority actinides that can be used in accelerator-driven subcritical systems, includes isotopes of thorium, uranium and plutonium. The majority of experimental data are available for ^{238}U. For this reason, ^{238}U is the best candidate for testing the models developed for nuclear data evaluations at intermediate energies.

The main results of experimental data analysis and calculations recommended for the intermediate energy neutron data file of ^{238}U are briefly discussed below. The corresponding file is in preparation now in the IPPE and evaluations accepted are labeled with IPPE-99 in the figures of the present work.

II. INCIDENT NEUTRON ENERGIES BELOW 20 MeV

Below 20 MeV the evaluations of BROND-2, ENDF/B-VI and JENDL-3.2 for ^{238}U give comprehensive and sufficiently accurate estimation of all neutron data required for fast reactors. Some possible improvements of the inelastic scattering cross sections for the low-lying collective levels were proposed recently by Maslov et al. [7], who took also into account, in coupled-channels calculations, levels of the γ band ($K^{\pi} = 2^{+}$) and of the octupole band ($K^{\pi} = 0^{-}$), with transition matrix elements computed in the frame of a soft rotor model.

In any case, good agreement of all evaluations is a reasonable guarantee for their applicability to accelerator-driven systems too.

III. INCIDENT NEUTRON ENERGIES ABOVE 20 MeV

Evaluations above 20 MeV are based on nuclear model calculations, whose parameters are to be adjusted on the available experimental data. A coupled-channels optical model is used to calculate the transmission coefficients for neutrons and charged particles, and to evaluate the angular distributions for neutron scattering as well.

The GNASH code [8] was used to calculate the integral and double differential cross sections and to prepare data in ENDF/B-VI format. The level density description for all channels was obtained on the basis of the generalized superfluid model fitted to experimental data on the density of low-lying discrete levels and neutron resonances. The phenomenological systematics of the level density parameters developed in the framework of the RIPL project [9] were applied to the fission channels and to nuclei for which the corresponding experimental information does not exist.

IIIA. Total and scattering cross sections

Evaluations of neutron total cross sections are based on coupled-channels optical model calculations with potential parameters fitted to experimental data. The analysis of such data was performed in many laboratories, and the deformed optical model parameters

obtained were used for the neutron cross section evaluations of actinides [7,10-12]. These sets of parameters give approximately the same total cross sections. However, the calculated neutron absorption cross sections differ significantly for various sets. Discrepancies of the absorption cross section evaluations are essential at neutron energies above 10 MeV, and their effects appear in the evaluated cross sections of (n,xn), fission and other reactions.

An optimal set of optical model parameters has been estimated from the analysis of experimental data of neutron total cross sections, angular distributions for proton elastic scattering and proton absorption cross sections. These parameters, shown in T. I, are close to those used for the intermediate energy neutron cross section evaluations of lead isotopes [13, 14].

The total cross section calculated with the parameters given above is compared in F. 1 with available experimental data and other calculations. Below 20 MeV there are many experimental data and only some of them are presented in . 1. A reasonable agreement of our calculations with the Barashenkov's systematics [15] and experimental data [16-21] is obtained for all energies above 20 MeV.

The corresponding calculations of neutron elastic scattering and absorption cross sections are shown in F. 2 and 3, respectively. There are no direct measurements of these cross sections at high energies. However, a reasonable estimation of them is given by Barashenkov's systematics, based mainly on proton reaction data [15]. The experimental data available for heavy nuclei are shown in F. 4 in comparison with the systematics [15] and our optical model calculations. The optical model calculations reproduce well the proton absorption cross section in the whole energy region from the Coulomb barrier to 200 MeV, and at high energies they are in reasonable agreement with the Barashenkov evaluations for both protons and neutrons. The necessity to reduce the absorption cross section at 200 MeV by about 20% with respect to the one calculated with the optical model parameters [6] was noted in the RIPL library summary too [12]. Therefore, the present evaluation of the absorption cross section above 100 MeV appears to be most consistent with all available experimental data.

The coupled-channels model makes it possible to calculate also the cross sections and angular distributions for elastic and inelastic scattering of neutrons with excitation of low-lying collective levels in the whole energy range. Experimental data of elastic scattering angular distributions are available only at incident neutron energy up to 14.1 MeV. Our calculations are compared with these data in F. 5. The contributions of the lowest collective levels, 2^+, 4^+ and 6^+, to inelastic scattering are shown, too. These levels are to be taken into

account because their excitation energies are much smaller than the energy resolution in the experimental data of elastic scattering. The quasi-elastic scattering angular distribution including the contributions of the low-lying collective levels is represented by the thick solid curve in F. 5. The reasonable agreement of calculations with experimental data allow us to apply the optical model to the evaluation of the elastic and inelastic scattering angular distributions for all higher energies. The results of such calculations are shown in F. 6 and 7 for the energies of 50 and 100 MeV, respectively. Unfortunately, there are no measurements of the neutron elastic scattering angular distributions for high energies.

IIIB. Fission cross sections and fission prompt neutrons

The fission cross section above 20 MeV was measured by several groups [26-30]. In our opinion, the experimental data of Pankratov [26] in the energy region from 20 to 40 MeV seem too high. The values of the LANL measurements reprocessed recently by Carlson [28] are accepted as the most reasonable in the whole energy region from 20 to 150 MeV. Data of Ref. [30] have a preliminary status and they should be taken in careful consideration only after the complete processing of measurement results.

The calculated fission cross section was fitted to the ENDF/B-VI evaluation, considered as the neutron standard at energies below 20 MeV, in order to obtain the fission barrier parameters. For higher energies, the effects of nuclear viscosity were included in the calculations of the fission widths of highly excited compound nuclei [31]. Since the observed fission cross section at high energies is determined by the contributions of more than a dozen residual nuclei, which undergo fission after emission of neutrons, or protons, an estimation of the fission barriers for all nuclei is a rather cumbersome task. Taking into account the damping of shell effects at high energies we confined the calculations by fitting the liquid drop barriers only. The final evaluation of the fission cross sections for energies above 20 MeV was obtained in the frame of a statistical approximation based on rational functions of the available experimental data and theoretical model curves. The result of such an approach, matched with the ENDF/B-VI evaluation at energies below 20 MeV, is shown in F. 8 together with the experimental data. An accurate description of the fission cross sections is very important for consistent evaluation of multiple emission of neutrons and charged particles.

The results of our evaluation for $<\nu>$, the average number of prompt neutrons per fission, are shown in F. 9 in the energy region up to 150 MeV together with the experimental data of Fréhaut [32] and the INPE evaluation below 50 MeV [33]. The evaluation is based on the Cascade Evaporation Fission Model calculations fitted to the experimental data below 50

MeV. In the upper part of F. 9 the corresponding temperature of the Maxwellian fission neutron spectrum is shown as a function of the incident neutron energy.

IIIC. Neutron production cross sections and spectra

Evaluations of particle emission spectra and corresponding production cross sections are performed in accordance with the rules of the ENDF/B-VI format for the double-differential cross sections, by using the Kalbach representation of such data [34]. Differential cross sections are described in this approach by the integral production cross section for the corresponding emitted particle multiplied by a normalized angular distribution function of the following form

$$f(m_b, E_a, E_b) = f_0(E_a, E_b)\left\{\frac{a(E_a, E_b)}{\sinh a(E_a, E_b)}\left[\cosh\left(a(E_a, E_b)m_b\right) + r(E_a, E_b)\sinh\left(a(E_a, E_b)m_b\right)\right]\right\},$$

where E_a is the incident particle energy in the laboratory system, m_b is the scattering angle cosine of the emitted particle b and E_b is its energy in the center-of-mass system, $f_0(E_a,E_b)$ is the normalized spectrum of the emitted particle, $r(E_a,E_b)$ is the pre-compound fraction of this spectrum, and $a(E_a,E_b)$ is the simple function proposed in Ref. [34], which depends mainly on the center-of-mass emission energy E_b and, to a lesser extent, on particle type and incident energy at higher values of E_a . In accordance with such a description, the two energy-dependent functions $f_0(E_a,E_b)$ and $r(E_a,E_b)$ determine completely the shape of emitted particle spectra and the anisotropy of the corresponding angular distributions, respectively.

Neutron emission is a dominant reaction that competes with nuclear fission. The calculated neutron production cross section is shown in F. 10. Below 20 MeV these calculations agree well enough with the evaluations of the (n,2n) and (n,3n) reactions based on experimental data and included in the files of BROND-2 or ENDF/B-VI. Above 20 MeV, there are no direct experimental data on neutron emission cross sections or on the multiplicity of secondary neutrons, which can be evaluated as the ratio of the calculated neutron production cross section to the reaction cross section considered above.

The calculated normalized spectra of emitted neutrons are shown in F. 11 for incident neutron energies from 20 to 150 MeV. The pre-equilibrium components of spectra become larger with increasing incident neutron energy, while the soft equilibrium components change only a little. The calculated r-factors that define the anisotropy of secondary neutron angular distributions are given in F. 12 for several incident neutron energies.

IIID. Charged particle emission cross sections and spectra

In order to calculate the transmission coefficients for protons, we used the same potential as for neutrons, with the corresponding Lane components. The calculated absorption cross section for such a potential agrees rather well with Barashenkov's systematics of the proton induced reaction cross sections at high energies [15], but, at the present time, the experimental data are not accurate enough to test such calculations for energies close to the Coulomb barrier.

The proton production cross section calculated with such transmission coefficients is shown in F. 13. The corresponding normalized proton spectra and r-factors are presented in F. 14 and 12, respectively.

For similar calculations of deuteron, triton and α-particle yields, which should be lower than the proton yields, we used the spherical optical model with the parameters given in Tables II, III and IV, respectively.

Some shortcomings of the preequilibrium model used in the GNASH code were demonstrated in the analysis of production cross sections of deuterons and heavier charged particles[14,38,39]. To get more accurate evaluations of deuteron, triton and α-particle yields, use was made of the modified ALICE-IPPE code, which describes the duster emission on the basis of the Ivamoto-Harada model [38] with parameters adjusted on the available experimental data of cluster yields and spectra in proton induced reactions [39]. Deuteron emission was calculated using the quasi-direct and pick-up mechanisms. For triton emission the pick-up processes were taken into account, and for α-particles the knock-out, pick-up and multiple preequilibrium emission were included into consideration.

The cross sections for the ^{238}U(n,xd), ^{238}U(n,xt) and ^{238}U(n,xα) reactions calculated in such an approach are shown in F. 15-17. The experimental data on the yields of the same charged particles in the proton induced reactions on ^{209}Bi and ^{232}Th, the heaviest studied targets, are shown for the sake of comparison. Undoubtedly, uncertainties of such estimations of light cluster production cross sections are rather large, but we do not have enough experimental data to improve the theoretical description significantly at the present time. On the other hand, all of these cross sections are much lower than the neutron production cross section and big uncertainties of less important cross sections seem acceptable for most applications related to the development of accelerator-driven systems.

To evaluate the spectra and angular distributions of emitted charged particles we returned, nevertheless, to the GNASH calculations, but the main parameter of the pre-

equilibrium model was changed for each cluster channel to obtain the same production cross sections as with the ALICE-IPPE code. The calculated spectra of deuterons, tritons and α-particles are shown in F. 18, 19 and 20, respectively. The corresponding ѓ-factors that define pree-quilibrium components of charged particle spectra are given in F. 21 for several energies of incident neutrons.

IV. SUMMARY AND CONCLUSIONS

The major components of the intermediate-energy neutron data evaluations for ^{238}U have been described in the present work. Evaluations are based on the coupled-channels model and the statistical model of pre-equilibrium and equilibrium particle emission, with theoretical model parameters adjusted on the available experimental data. The recommended values are matched up with the well tested data below 20 MeV and can be used for preparation of the complete neutron data file of ^{238}U.

ACKOWLEDGMENT

The present work was supported in part by ENEA Contract No. 98-59-00868-73. We wish to thank the ENEA-ADS project leader, Dr. G. Gherardi, for permanent interest in this work and fruitful discussions.

REFERENCES

1. A.J.Koning, "Requirements for an Evaluated Nuclear Data File for Accelerator Based Transmutation," Report NEA/NSC/DOC(93)6 and ECN-C-93-005; "Nuclear Data Evaluation for Accelerator-Driven Systems," in *Proc. Second International Conference on Accelerator-Driven Transmutation Technologies and Applications*, Kalmar, Sweden, June 3-7, 1996, Vol. 1, p. 438, H. Condé, Ed., Gotab, Stockholm, Sweden (1997).
2. H.W.Bertini, "Intranuclear-Cascade Calculation of the Secondary Nucleon Spectra from Nucleon-Nucleus Interactions in the Energy Range 340-2900 MeV and Comparison with Experiment," *Phys.Rev*. **188,** 1711 (1969).

3. V.S.Barashenkov, V.D.Toneev, Interactions of High Energy Particles with Nuclei (Atomizdat, Moscow, 1972).
4. R.E.Prael, H.Lichtenstein, "Users Guide to the LAHET Code System," Report LA-UR-89-3014, Los Alamos National Laboratory (1989).
5. M.B.Chadwick, P.G.Young, S.Chiba, S.C. Frankle, G.M. Hale, H.G. Hughes, A.J. Koning, R.C. Little, R.E. MacFarlane, R.E. Prael, and L.S. Waters, "Cross-Section Evaluations to 150 MeV for Accelerator-Driven Systems and Implementation in MCNPX," *Nucl. Sci. Eng.* **131**, 293 (1999).
6. P.G.Young, E.D.Arthur, M.Bozoian, T.R.England, G.M. Hale, R.J.LaBauve, R.C. Little, R.E.MacFarlane, D.G.Madland, R.T.Perry, and W.B.Wilson, "Transport Data Libraries for Incident Proton and Neutron Energies to 100 MeV," Report LA-11753-MS, Los Alamos National Laboratory (1990).
7. V.M.Maslov, Yu.V.Porodzinski, A.Hasegawa, K.Shibata, "New Evaluations of Neutron Cross Sections for ^{238}U," Report JAERI-Research-98-040, 1998.
8. P.G.Young, E.D.Arthur, M.B.Chadwick, "Comprehensive Nuclear Model Calculations: Theory and Use of the GNASH Code," in *Proc.IAEA Workshop on Nuclear Reaction Data and Nuclear Reactors Trieste, Italy, 15 April - 17 May 1996*, Vol. 1, p. 227, A.Gandini and G.Reffo Editors, World Scientific, Singapore (1998)
9. A.V.Ignatyuk, "Level Densities," in Reference Input Parameter Library for Nuclear Model Calculations – Handbook, IAEA – TECDOC-1034, Vienna, 1998, ch. 5.
10. L.F.Hansen, B.A.Pohl., C.Wong, R.C.Haight, Ch.Lagrange, "Measurements and Calculation of Neutron Scattering in Actinide Region," *Phys. Rev.* **C34**, 2075 (1986).
11. V.A.Konshin, "Calculations of Neutron and Proton Induced Reaction Cross Sections for Actinides in the Energy Region from 10 MeV to 1 GeV," Report JAERI-Research-95-036, Japan Atomic Energy Research Institute (1995).
12. P.G.Young, "Optical Model Parameters," in Reference Input Parameter Library for Nuclear Model Calculations – Handbook, IAEA–TECDOC-1034, Vienna, 1998, ch. 4.
13. H.Vonach, A.Pavlik, M.B.Chadwick, R.C. Haight, R.O. Nelson, S.A. Wender, and P.G. Young, "$^{207,\ 208}$Pb(n,xn) Reactions for Neutron Energies from 3 to 200 MeV," *Phys. Rev.* **C50**, 1952 (1994).
14. M.B.Chadwick, P.G.Young, "GNASH Calculations of the Neutron and Proton Induced Reactions for Lead Isotopes and Benchmarking of Results," Report T-2-96, Los Alamos National Laboratory (1996).

15. V.S.Barashenkov, Cross Sections of Particle and Nucleus Interactions with Nuclei (Russian), JINR, Dubna, 1993.
16. W.I. Linlor, B. Ragent," Neutron Total Cross Sections for Bismuth and Uranium between 45 and 160 MeV," *Phys. Rev* **92**, 835 (1953).
17. P.H. Bowen, J.P. Scanlon, G.H. Stafford, J.J. Thresher, P.E. Hodgson, Neutron Total Cross-Sections in the Energy Range 15 to 120 MeV. *Nucl.Phys.*, **22 ,** 640 (1961).
18. R.J. Schneider, A.M. Cormack, "Neutron Total Cross Sections in the Energy Range 100 - 150 MeV," *Nucl. Phys.* **A119**, 197 (1968).
19. D.G.Foster Jr, D.W.Glasgow. "Neutron Total Cross Sections, 2.5-15 MeV. I. Experimental," *Phys. Rev*. **C3,** 576 (1971).
20. W.P.Poenitz, J.F.Whalen., "Neutron Total Cross Section Measurements in the Energy Region from 47 keV to 20 MeV," Report ANL-NDM-80 (1983).
21. J.J.Franz, H.P.Grotz, L.Lehmann, E.Roessle, H.Schmitt, L.Schmitt, "Total Neutron-Nucleus Cross Sections at Intermediate Energies," *Nucl. Phys.* **A490**, 667 (1988).
22. J.Voignier, "Study of Interaction of 14 MeV Neutrons with U-238," Report CEA-R-3503 (1968)
23. W.Bucher, C.E.Hollandsworth, J.E.Youngblood, "Small-Angle Scattering of Fast Neutrons," *Phys. Rev. Lett.* **35**, 1419 (1975).
24. Shen Guanran, Huang Tangzi, Wen Shenlin,Yu Chunying, Li Anli,Tang Hongoing, Shen Qingbiao, Zhao Zhixinag, Gu Fuhua, "Fast Neutron Elastic Scattering Differential Cross Sections from U-238," *Chinese J. Nucl. Phys.* **6,** 193 (1984).
25. L.F.Hansen, B.A.Pohl, C.Wong, R.C.Haight., Ch.Lagrange, "Measurements And Calculation of Neutron Scattering in the Actinide Region," *Phys. Rev*. **C34**, 2075 (1986).
26. V.M. Pankratov, "Fission Cross Sections of Th-232, U-233, U-235, Np-237, U-238 for 5-37 MeV Neutrons," *Atomnaya Energia*, **14**, 177 (1963).
27. P.W.Lisowski et al., in *Proc. Symp. on Neutron Cross-Sections from 10 to 50 MeV*. Upton, 1980, Vol. 1, p.301; in *Proc. Specialists' Meeting on Neutron Cross-Sections Standards for the Energy Region above 20 MeV* (Uppsala, May 1991), NEANDC-305/U, p.177 (1991)
28. A.Carlson, "Neutron Induced Fission Cross Sections U-235 and U-238 above 20 MeV", Report to Consultants'Meeting on Nuclear Data Standards for Nuclear Measurements (Vienna, December 1996), IAEA, Vienna, INDC(NDS)-368 (1997).

29. V.P.Eismont, A.V.Prokofyev, A.N.Smirnov et al., "Relative and absolute neutron-induced fission cross sections of ^{208}Pb, ^{209}Bi, and ^{238}U in the intermediate energy region," *Phys.Rev.* **C53,** 2911 (1996).
30. A.Yu.Donets, A.V.Evdokimov, A.V.Fomichev, T.Fukahori, A.B.Laptev, G.A.Petrov, O.A.Shcherbakov, Yu.V.Tuboltsev, A.S.Vorobyev, "Neutron Induced Fission Cross-Sections of ^{233}U, ^{235}U, ^{238}U, ^{232}Th, ^{239}Pu, and ^{237}Np in the Energy Range 1 - 200 MeV," in: *Proceedings of VII International Seminar on Interaction Neutrons with Nuclei,* (Dubna, 1999, to be publ.)
31. A.V.Ignatyuk, G.A.Kudyaev, A.R.Junghans, M.deJong, M.G.Clerc, and K.H.Schmidt, "Analysis of dissipation effects in nuclear fission observed in the fragmentation of ^{238}U projectiles," *Nucl. Phys*. **A593**, 519 (1995).
32. J.Fréhaut, "Nu-bar Results at Bruyères-le-Châtel", Private communication to EXFOR-21685 (1976).
33. Yu.A.Korovin, A.Yu.Konobeev, V.P.Lunev, P.E.Pereslavtsev, A.Yu.Stankovski, "Evaluated Data File for U-238," Obninsk, Institute of Nuclear Power Engineering (1996).
34. C.Kalbach, "Systematics of Continuum Angular Distributions," *Phys. Rev*. **C37,** 2350 (1988).
35. J.Bojowald, H.Machner, H.Nann, W.Oelert, M.Rogge, and P.Turek, "Elastic deuteron scattering and optical model parameters at energies up to 100 MeV," *Phys. Rev*. **C38,** 1153 (1988).
36. F.D.Becchetti Jr, and G.W.Greenlees. Ann. Rep. J.H. Williams Lab., Univ. Minnesota (1969).
37. V.Avrigeanu, P.E.Hodgson, and M.Avrigeanu, "Global Optical Potentials for Emitted Alpha Particles," *Phys.Rev*. **C49,** 2255 (1994).
38. A.Iwamoto, K.Harada, "Mechanism of Cluster Emission in Nucleon-Induced Preequilibrium Reactions," *Phys. Rev*. **C26,** 1821 (1982).
39. A.I.Dityuk, A.Yu.Konobeyev, V.P.Lunev, Yu.N.Shubin. "New Advanced Version of Computer Code ALICE-IPPE," Report INDC(CCP)-410, IAEA, Vienna (1998).
40. F.E.Bertrand and R.W.Peelle,"Complete Hydrogen and Helium Particle Spectra from 30 to 60 MeV Proton Bombardment of Nuclei with A=12 to 209 and Comparison with Intranuclear Cascade Model," *Phys. Rev*. **C8**, 1045 (1973).
41. J.R.Wu, C.C.Chang , H.D.Holmgren, "Charged particle spectra: 90 MeV Protons on ^{27}Al, ^{58}Ni, ^{90}Zr, and ^{209}Bi," *Phys. Rev*. **C19,** 698 (1979).

42. M. Lefort, G.N. Simonoff, X. Tarrago, R.Bibron, " Production de Tritium dans le Thorium par des Protons de 135 MeV," *J Phys. Radium*, **20** ,959 (1959).
43. C. Brun, M.Lefort, X.Tarrago, "Contribution a l'Etude du Double Pick-up Indirect Mesure de la Production de Tritium par des Protons de 82 et 105 MeV dans Diverses Cibles," *J. Phys. Radium*, **23,** 167 (1962).
44. M. Lefort, J.P. Cohen, H. Dubost, and X. Tarrago, "Evidence for Nucleon Clustering from High-Energy Reactions," *Phys. Rev*. **139B** , 1500 (1965).
45. H. Gauvin, M. Lefort, and X. Tarrago, "Emission d'Helions dans les Reactions de Spallation," *Nucl. Phys.* **39**, 447 (1962).
46. H. Dubost, M. Lefort, J. Peter, and X. Tarrago. "^{4}He and ^{3}He Particles from Au, Bi and Th Nuclides Bombarded by 157-MeV Protons," *Phys. Rev*. **136B** , 1618 (1964).

TABLE I. Optical potential parameters for neutrons and protons on ^{238}U*

Well depth, MeV	Energy Range, MeV	Geometry, fm
$V_r = 52.33 \pm 16\eta + 0.04306E - 0.02377E^2 + \Delta_c$ $V_r = 51.192 \pm 16\eta - 0.2085E + \Delta_c$ $V_r = 53.096 \pm 16\eta - 0.2377E + \Delta_c$	$0 < E < 14$ $14 < E < 65$ $65 < E < 150$	$r_v = 1.185, \quad a_v = 0.8$
$\Delta_c = 0.4Z/A^{1/3}$		$r_{coul} = 1.26$
$W_d = 3.082 \pm 8\eta + 0.8477E - 0.01924E^2$ $W_d = 11.1232 \pm 8\eta - 0.14882E$ $W_d = 8.067 \pm 8\eta - 0.08235E$	$0 < E < 10$ $10 < E < 50$ $50 < E < 150$	$r_d = 1.26, \quad a_d = 0.52$
$W_V = 0.0$ $W_v = -1.7843 + 0.12745E$ $W_v = 2.9792 + 0.05417E$	$0 < E < 14.4$ $14.4 < E < 65$ $65 < E < 150$	$r_v = 1.26, \quad a_v = 0.5 + 0.0125E$
$V_{so} = 6.18$	$0 < E < 150$	$r_{so} = 1.16, \quad a_{so} = 0.667$

*Here $\eta = (A-2Z)/A$; $\beta_2 = 0.23$, $\beta_4 = 0.045$ and the scheme of 0^+-2^+-4^+-6^+coupled levels is adopted.

TABLE II. The optical potential parameters for deuterons [35]

Well depth, MeV	Energy range, MeV	Geometry, fm
$V_r = 81.32 - 0.24E + \Delta_c$		$r_v = 1.18, \quad a_v = 0.636 + 0.035A^{1/3}$
$\Delta_c = 1.43Z/A^{1/3}$		$r_{coul} = 1.30$
$W_v = 0.0$ $W_v = 0.132(E-45)$	$E < 45$ $E > 45$	$r_{wv} = 1.27, \quad a_{wv} = 0.768 + 0.021A^{1/3}$
$W_d = \max(0; 7.80 + 1.04A^{1/3} - 0.712W_v)$		$r_{wd} = 1.27, \quad a_{wd} = 0.768 + 0.021A^{1/3}$
$V_{so} = 6.00$		$r_{so} = 0.78 + 0.038A^{1/3}$ $a_{so} = 0.78 + 0.038A^{1/3}$

TABLE III. The optical potential for tritons [36]

Well depth, MeV	Energy Range, MeV	Geometry, fm
V_r= 165.0 -0.17E -6.4(A-2Z)/A		r_v= 1.200, a_v= 0.720
		r_{coul}=1.30
W_v= 46.0 -0.33E -110(A-2Z)/A W_v= 32.8 -110(A-2Z)/A	E< 40 MeV E> 40 MeV	r_{wv}= 1.40, a_{wv}= 0.840
V_{so}= 2.5		r_{so}= 1.200, a_{so}= 0.720

TABLE IV. The optical potential parameters for α-particles [37]

Well depth, MeV	Energy range, MeV	Geometry, fm
V_r= 101.1-0.248E+Δ_c		r_v= 1.245; a_v=0.817-0.0085$A^{1/3}$
Δ_c= 6.051Z/$A^{1/3}$		r_{coul}=1.245
W_d= 12.64+0.2E -1.706$A^{1/3}$ W_d= 26.82+0.006E -1.706$A^{1/3}$	E<73 E>73	r_{wd}= 1.570, a_{wd}= 0.692

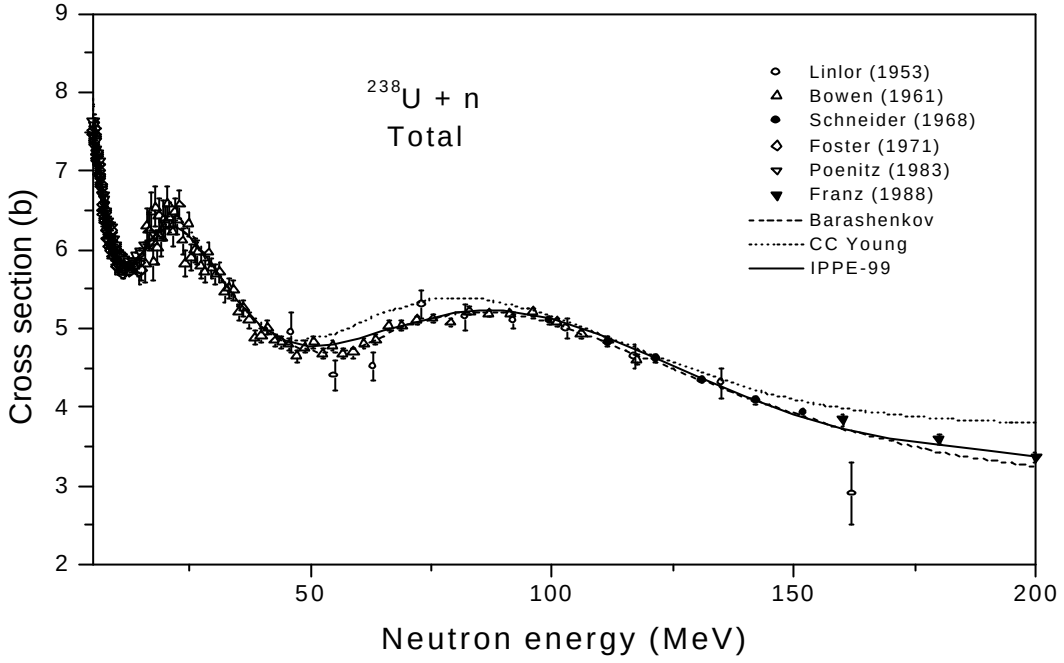

F. 1. Comparison of different calculations of the total neutron cross section with experimental data: Linlor et al. [16]; Bowen et al. [17]; Schneider et al. [18]; Foster at al. [19], Poenitz et al. [19], and Franz et al. [20].

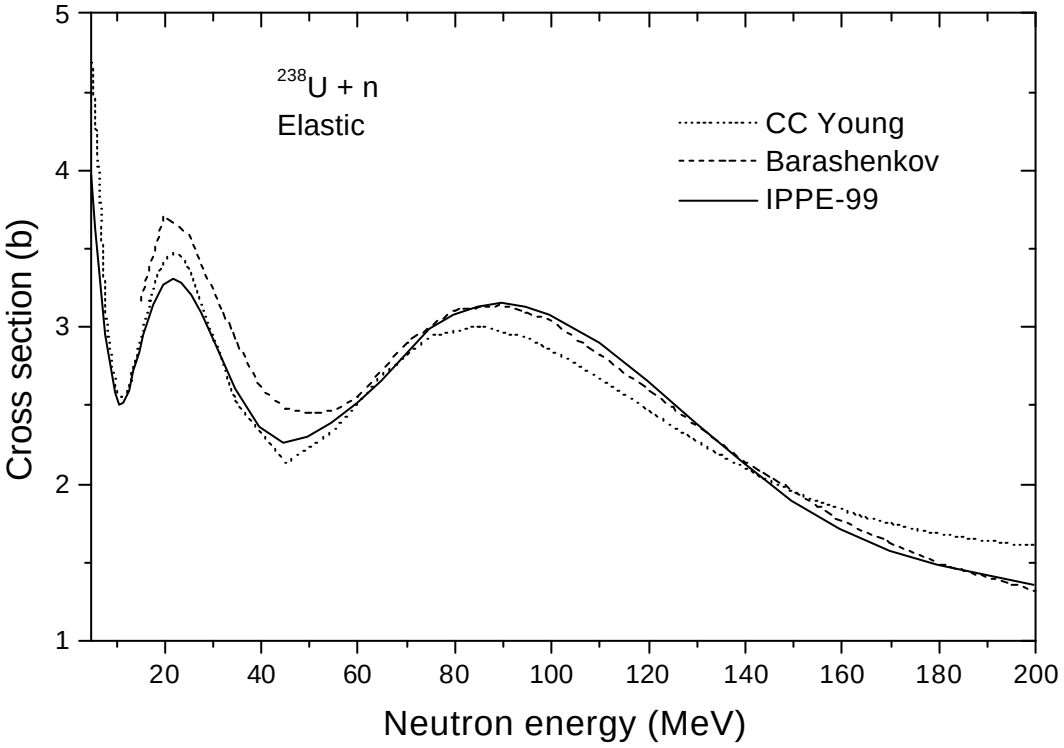

F. 2. Comparison of different calculations of the elastic neutron cross section.

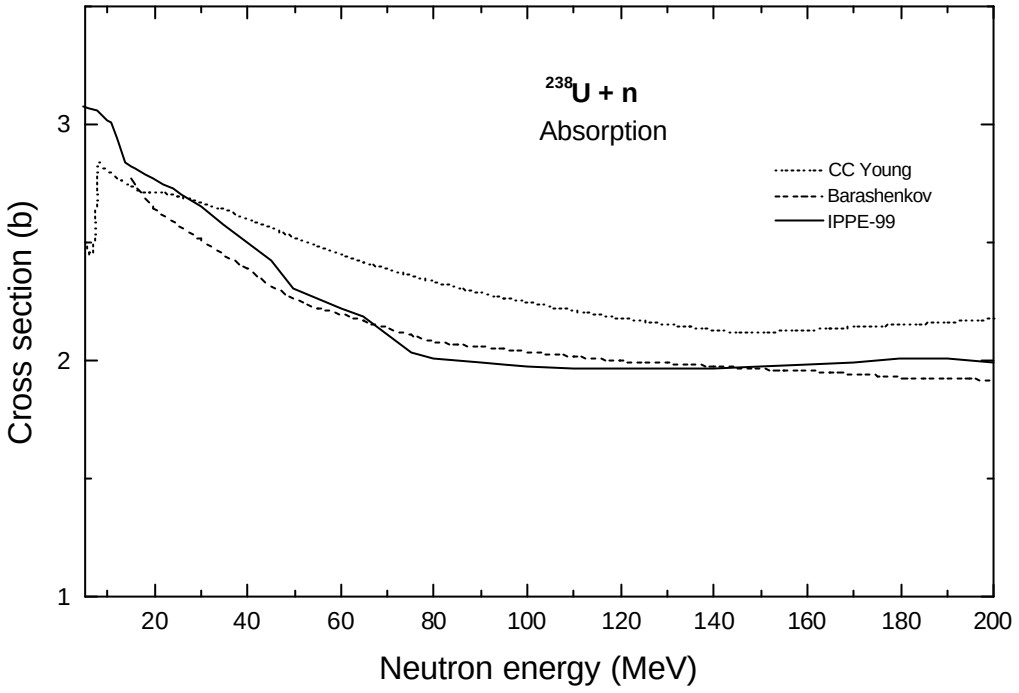

F. 3. Neutron absorption cross section calculated for different parameters of the deformed optical potential.

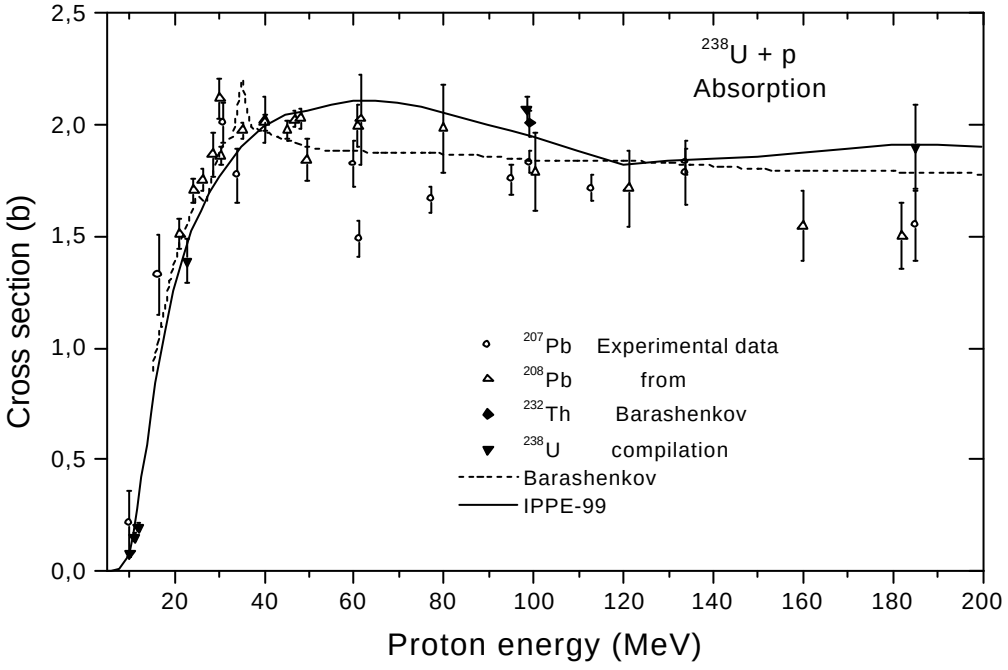

F. 4. Proton absorption cross section.

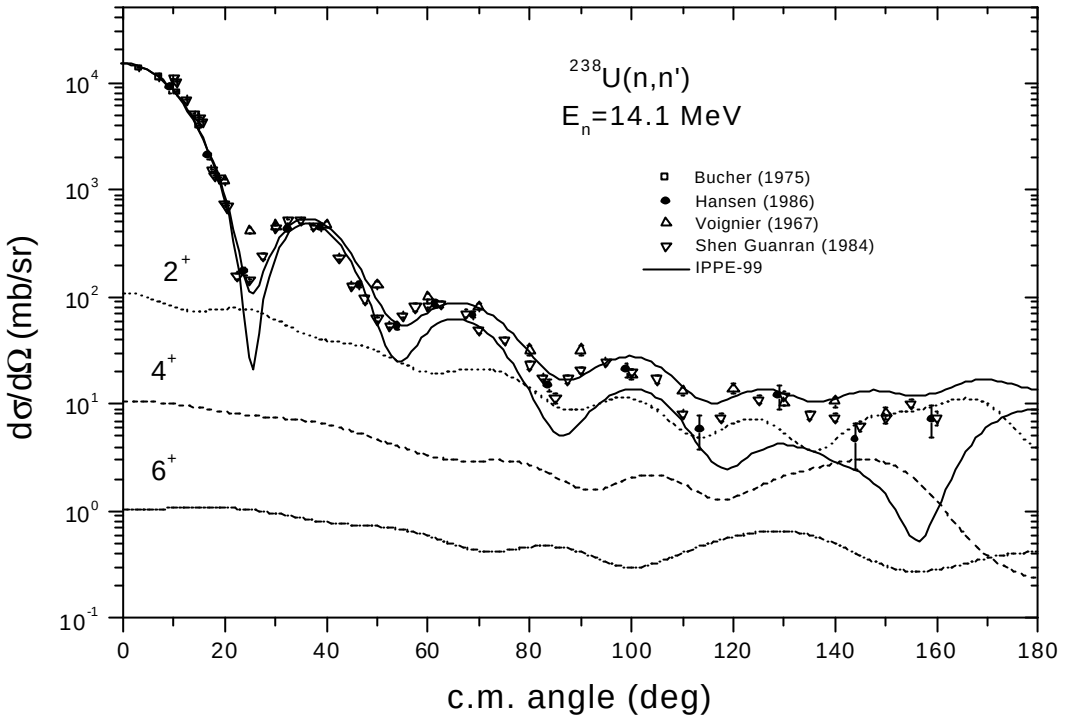

F. 5. Comparison of the calculated elastic scattering cross section at 14.1 MeV with experimental data. The scattering cross sections for the ground and collective low-lying levels are shown by solid, dotted dashed and dot-dashed curves respectively. The thick solid curve is the sum of the cross sections for the ground and collective low-lying levels; experimental references: Voignier et al. [22]; Bucher et al. [23]; Shen Guanran et al. [24]; Hansen et al. [25].

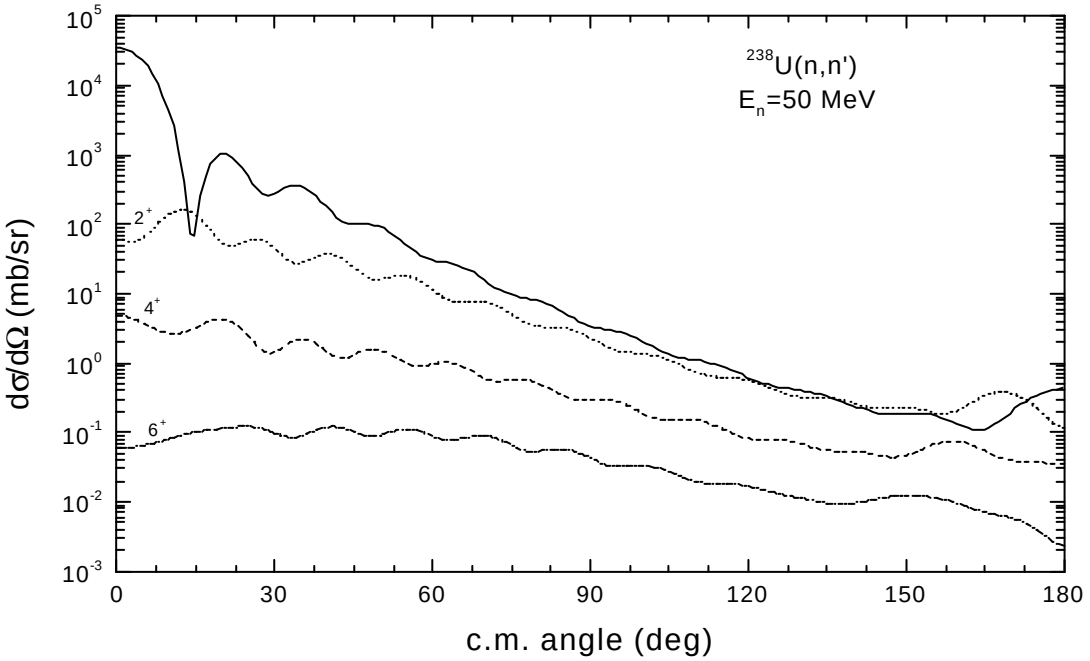

F. 6. Recommended elastic and inelastic scattering cross sections for ^{238}U at 50 MeV.

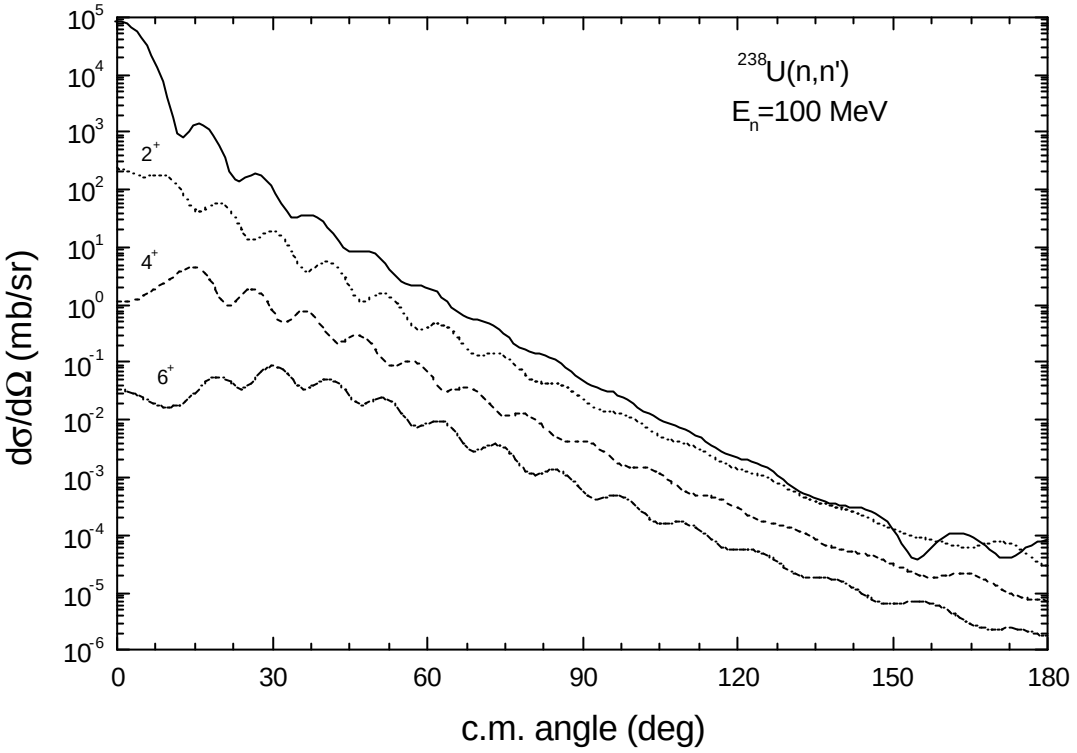

F. 7. Recommended elastic and inelastic scattering cross sections for ^{238}U at 100 MeV.

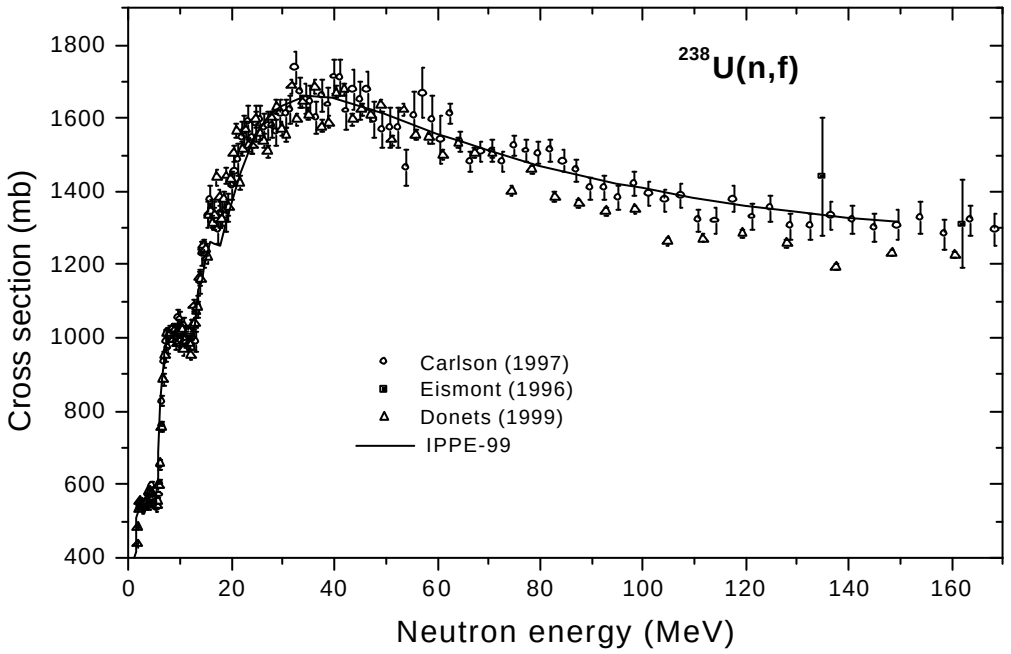

F. 8. Calculated fission cross section in comparison with experimental data by Carlson [28], Eismont et al. [29], and Donets et al. [30].

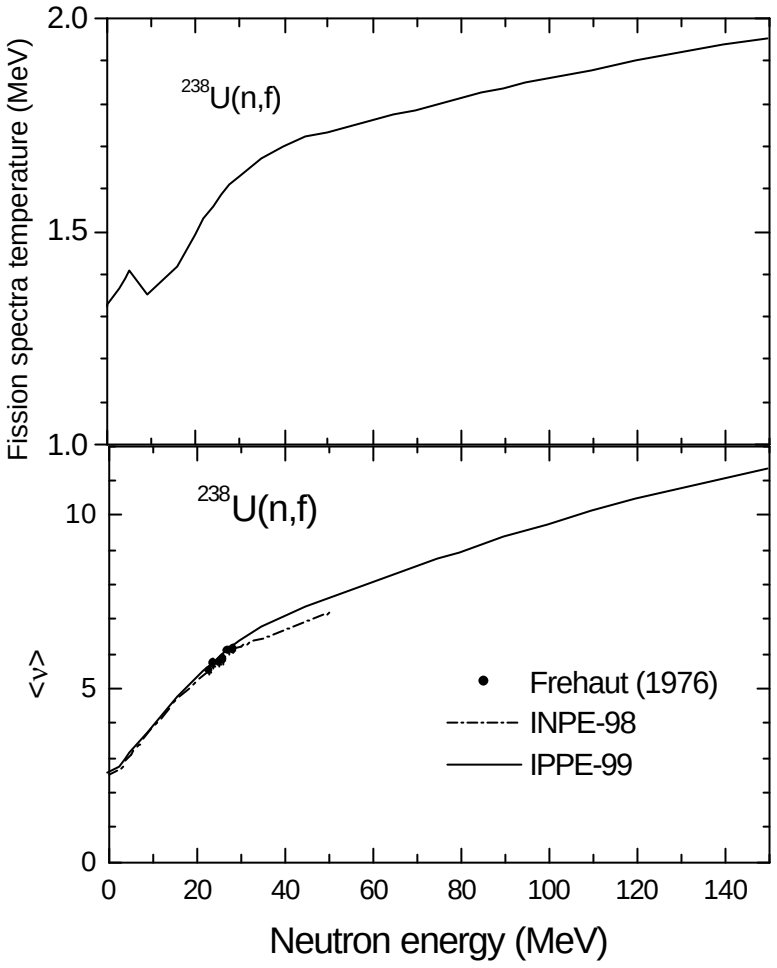

F. 9. Recommended prompt fission neutron number and fission neutron spectra temperature with the available above 20 MeV experimental data [32] and the IPPE evaluation [33].

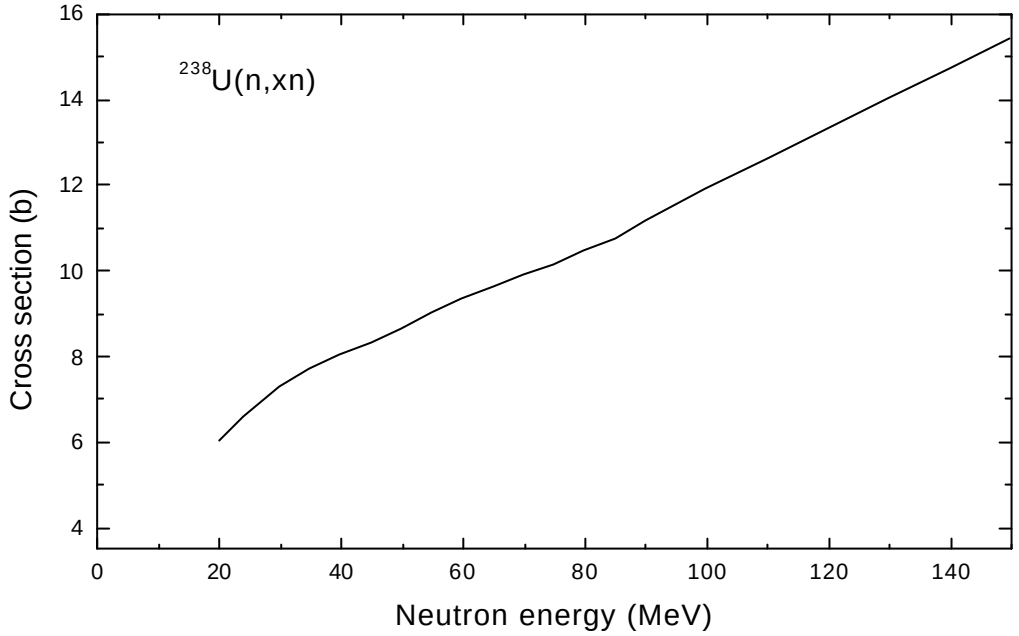

F. 10. Neutron production cross section calculated with GNASH.

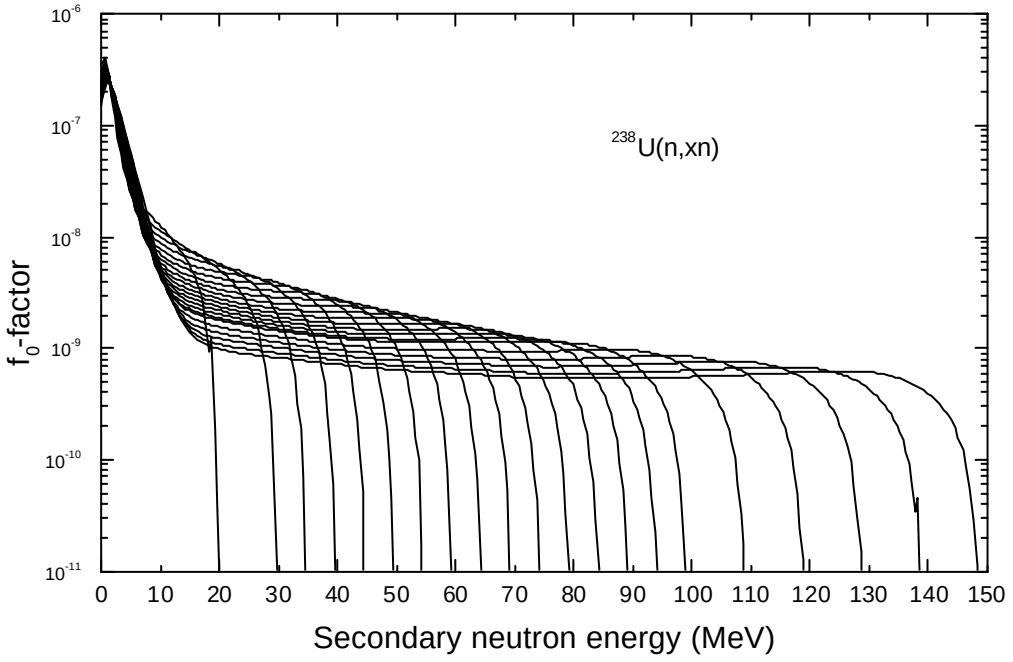

F. 11. Normalized secondary neutron spectra for the incident neutron energies from 20 to 150 MeV.

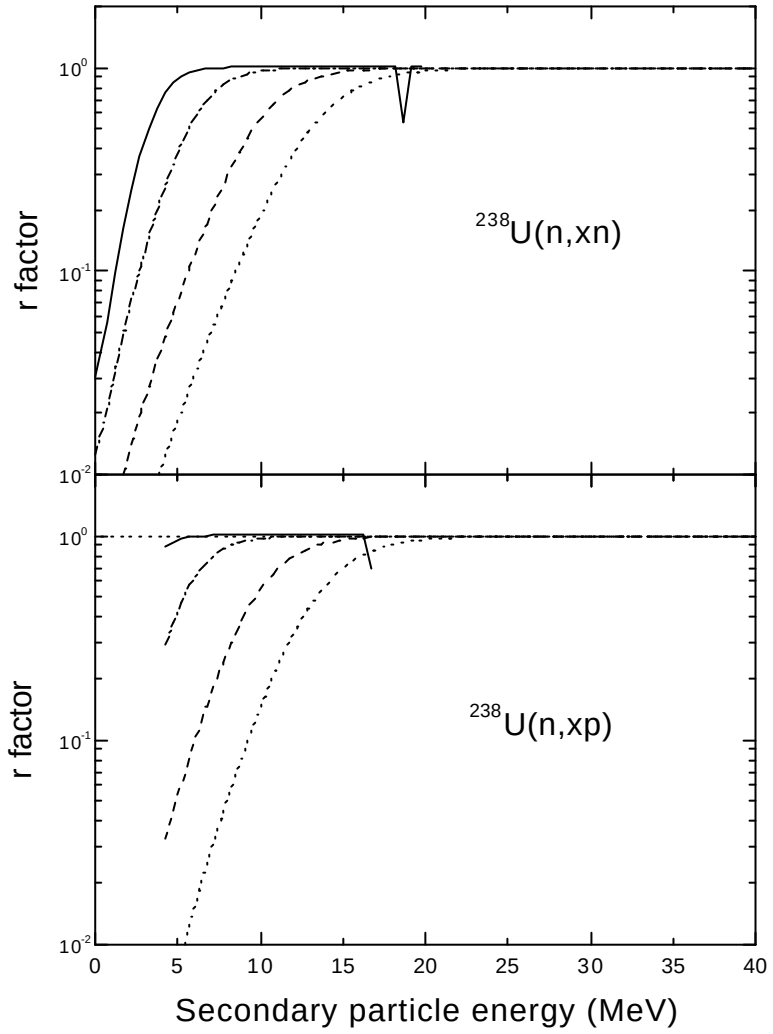

F. 12. Preequilibriuim components of the neutron and proton spectra for the incident neutron energies 20 MeV (solid), 50 MeV (dot-dashed), 100 MeV (dashed), and 150 Mev (dotted) curves.

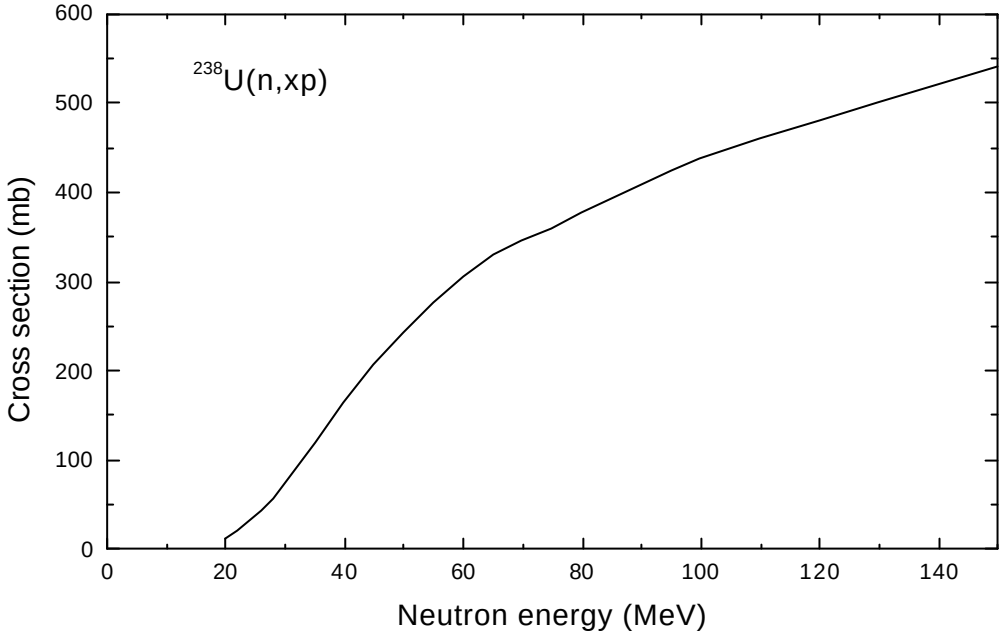

F. 13. The proton production cross section calculated with GNASH.

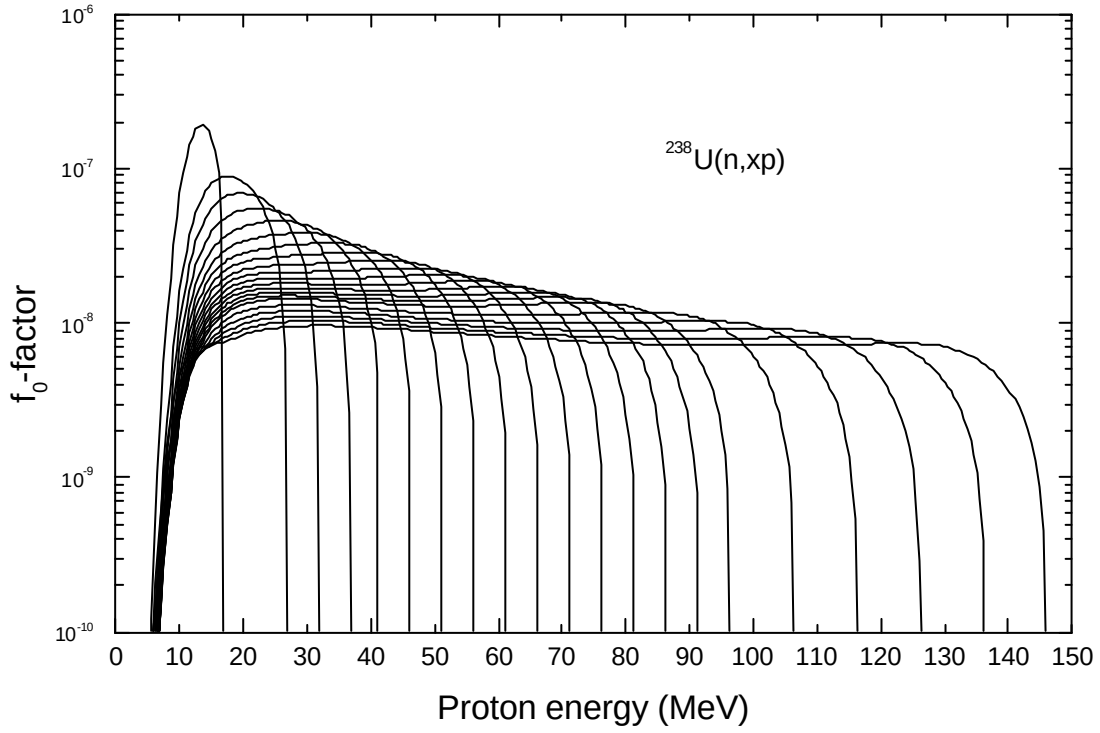

F. 14. Normalized secondary proton spectra for the incident neutron energies from 20 to 150 MeV.

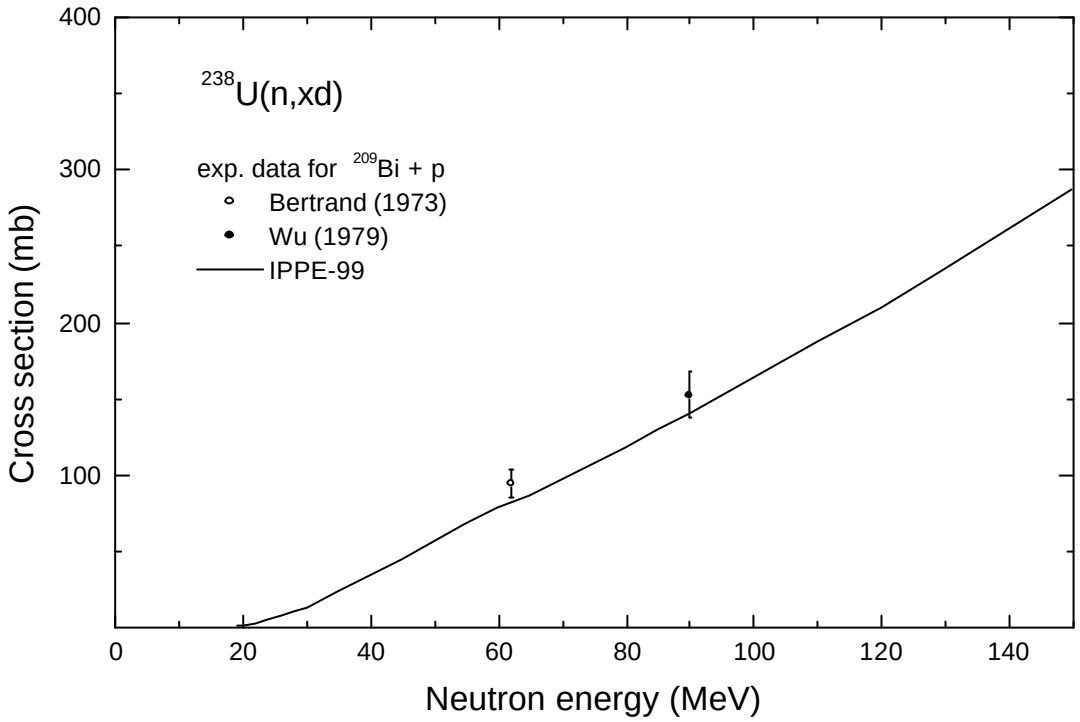

F. 15. The deuteron production cross section evaluated on the basis of statistical calculations and experimental data by Bertrand et al. [40] and Wu et al. [41].

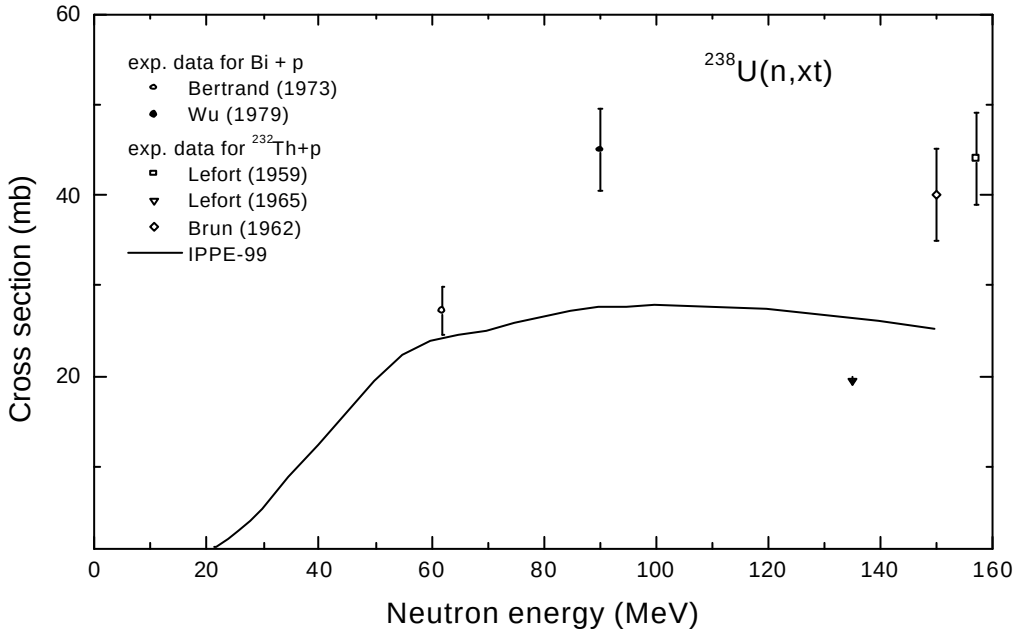

F. 16. The triton production cross section evaluated on the basis of statistical calculations and experimental data by Bertrand et al. [40], Wu et al. [41], Lefort at al. [42, 44], and Brun et al. [43].

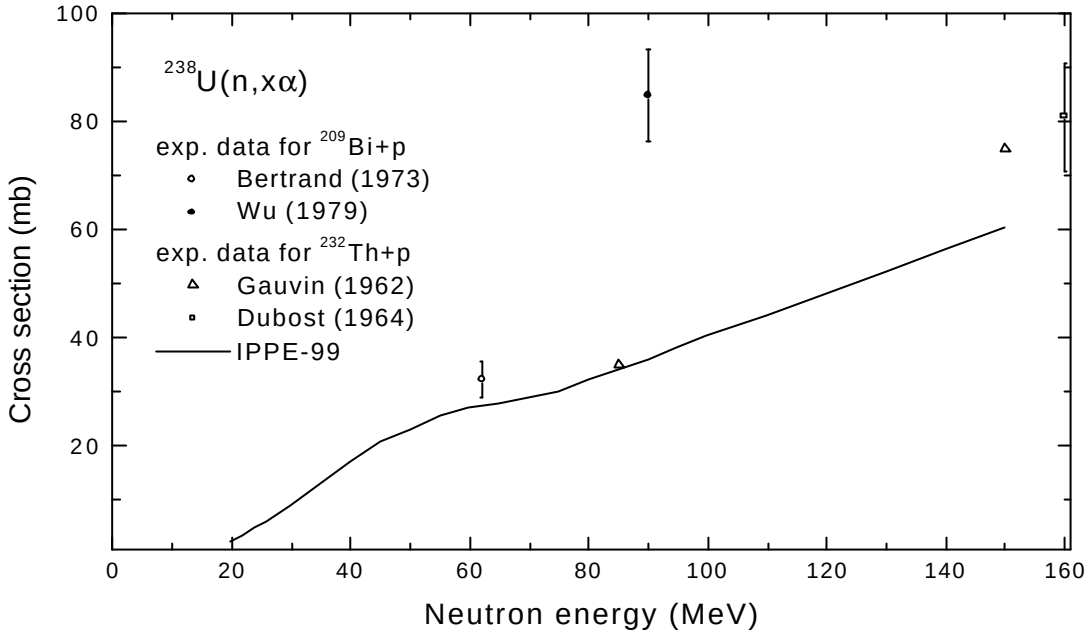

F. 17. The α-production cross section evaluated on the basis of statistical calculations and experimental data by Bertrand et al. [40], Wu et al. [41], Gauvin et al. [45], and Dubost at al. [46].

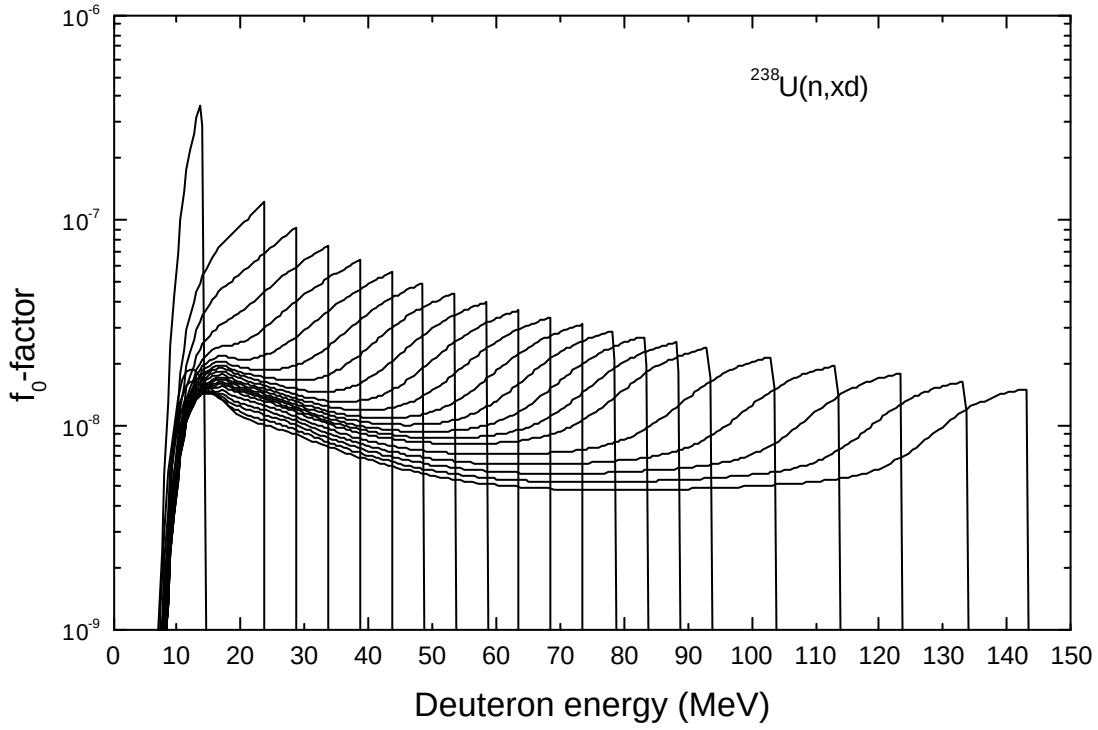

F. 18. Normalized secondary deuteron spectra for the incident neutron energies from 20 to 150 MeV.

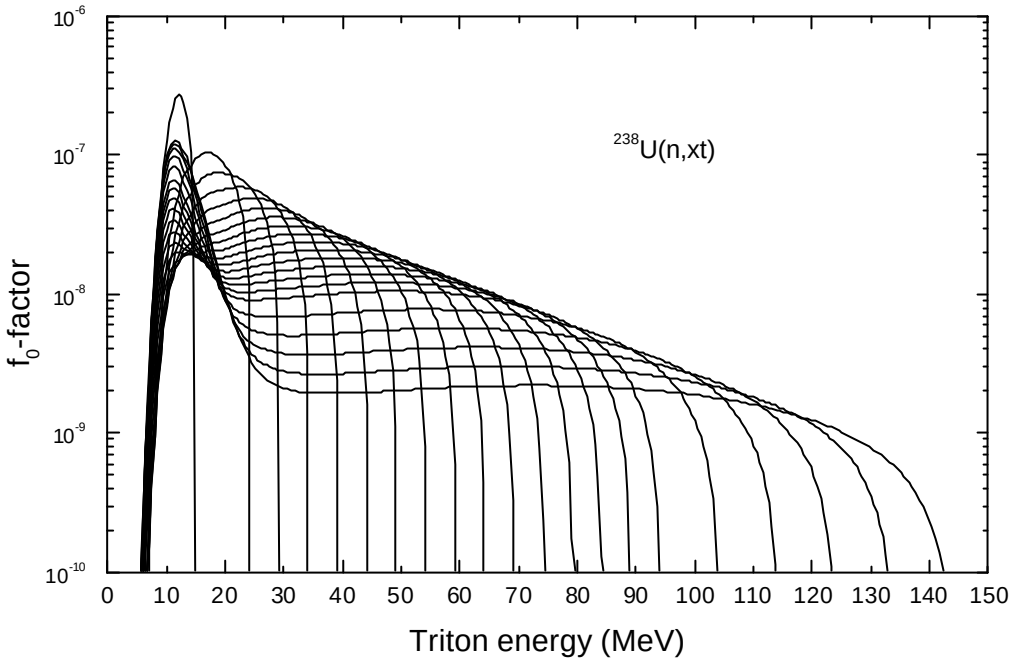

F. 19. Normalized secondary triton spectra for the incident neutron energies from 20 to 150 MeV.

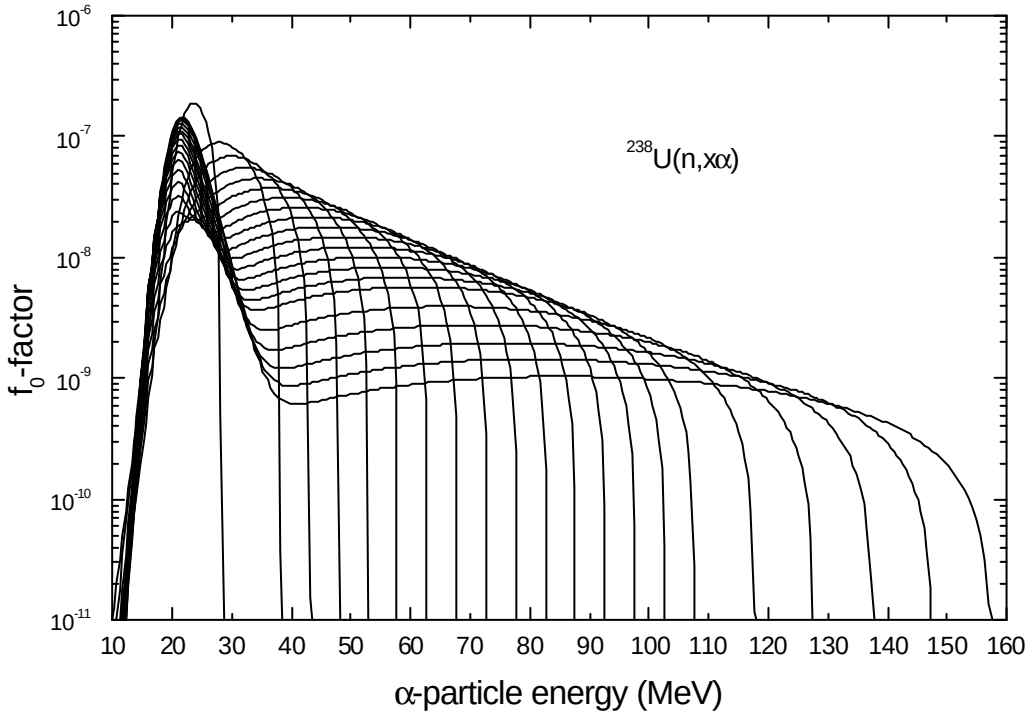

F. 20. Normalized secondary α-particle spectra for the incident neutron energies from 20 to 150 MeV.

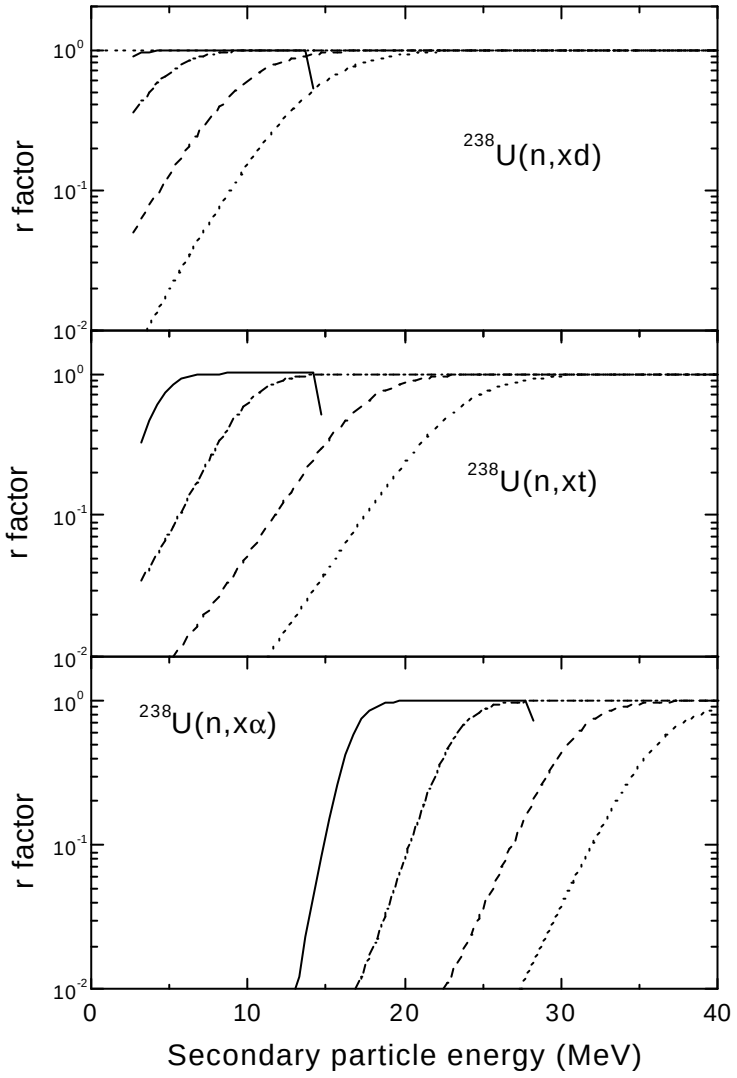

F. 21. Preequilibriuim components of the deuteron, triton and α-particle spectra for the incident neutron energies 20 MeV (solid), 50 MeV (dot-dashed), 100 MeV (dashed), and 150 Mev (dotted) curves.

CAPTIONS TO FIGURES:

F. 1. Comparison of different calculations of the total neutron cross section with experimental data: Linlor et al. [16]; Bowen et al. [17]; Schneider et al. [18]; Foster at al. [19], Poenitz et al. [19], and Franz et al. [20].

F. 2. Comparison of different calculations of the elastic neutron cross section.

F. 3. Neutron absorption cross section calculated for different parameters of the deformed optical potential.

F. 4. Proton absorption cross section.

F. 5. Comparison of the calculated elastic scattering cross section at 14.1 MeV with experimental data. The scattering cross sections for the ground and collective low-lying levels are shown by solid, dotted dashed and dot-dashed curves respectively. The thick solid curve is the sum of the cross sections for the ground and collective low-lying levels; experimental references: Voignier et al. [22]; Bucher et al. [23]; Shen Guanran et al. [24]; Hansen et al. [25].

F. 6. Recommended elastic and inelastic scattering cross sections for ^{238}U at 50 MeV.

F. 7. Recommended elastic and inelastic scattering cross sections for ^{238}U at 100 MeV.

F. 8. Calculated fission cross section in comparison with experimental data by Carlson [28], Eismont et al. [29], and Donets et al. [30].

F. 9. Recommended prompt fission neutron number and fission neutron spectra temperature with the available above 20 MeV experimental data [32]and the IPPE evaluation [33].

F. 10. Neutron production cross section calculated with GNASH.

F. 11. Normalized secondary neutron spectra for the incident neutron energies from 20 to 150 MeV.

F. 12. Preequilibriuim components of the neutron and proton spectra for the incident neutron energies 20 MeV (solid), 50 MeV (dot-dashed), 100 MeV (dashed), and 150 Mev (dotted) curves.

F. 13. The proton production cross section calculated with GNASH.

F. 14. Normalized secondary proton spectra for the incident neutron energies from 20 to 150 MeV.

F. 15. The deuteron production cross section evaluated on the basis of statistical calculations and experimental data by Bertrand et al. [40] and Wu et al. [41].

F. 16. The triton production cross section evaluated on the basis of statistical calculations and experi-mental data by Bertrand et al. [40], Wu et al. [41], Lefort at al. [42, 44], and Brun et al. [43].

F. 17. The α-production cross section evaluated on the basis of statistical calculations and experimental data by Bertrand et al. [40], Wu et al. [41], Gauvin et al. [45], and Dubost at al. [46].

F. 18. Normalized secondary deuteron spectra for the incident neutron energies from 20 to 150 MeV

F. 19. Nomalized secondary triton spectra for the incident neutron energies from 20 to 150 MeV.

F. 20. Normalized secondary α-particle spectra for the incident neutron energies from 20 to 150 MeV.

F. 21. Preequilibriuim components of the deuteron, triton and α-particle spectra for the incident neutron energies 20 MeV (solid), 50 MeV (dot-dashed), 100 MeV (dashed), and 150 Mev (dotted) curves.